Scaling exponents of sandpile-type models of self-organized criticality

S. D. Edney,* P. A. Robinson, and D. Chisholm
School of Physics, University of Sydney, New South Wales 2006, Australia
(Received 17 April 1998; revised manuscript received 24 June 1998)

Critical scaling exponents for eight sandpile-type systems that display self-organized criticality are determined numerically. These results are consistent with previous results where available and provide a more extensive, accurate, and consistent set of exponents than has previously been published for the set of models overall. Several theoretical interrelationships between the various exponents are verified.
[S1063-651X(98)09510-5]

PACS number(s): 64.60.Lx

I. INTRODUCTION

The concept of self-organized criticality (SOC) was introduced by Bak, Tang, and Wiesenfeld [1] to explain the frequent occurrence of $1/f$ noise in nature. Typically SOC occurs when a system driven toward instability reaches a critical state in which there is a statistical balance between driving and relaxation. This state exhibits sporadic relaxation via avalanches of energy release. These avalanches have a power-law distribution of sizes and establish power-law spatial and temporal correlations in the system. The SOC state is characterized by power-law distributions and corresponding scaling exponents of various physical quantities such as the size, duration, and total energy release of avalanches. The main purpose of this paper is to obtain improved estimates of scaling exponents of a range of SOC models in order to classify them into universality classes, test theoretical predictions, and provide improved values for use in applications.

The early systems used to study SOC behavior were models of sandpiles that were driven to instability by the addition of grains of sand and relaxed through slippage of sand down the pile when the local slope became too steep. Since then SOC has also been applied to various phenomena ranging from earthquakes [2] to solar flares [3] and mountain avalanches [4].

Kadanoff *et al.* [5] found that sandpile models lie within broad universality classes, with all models in a given class displaying the same scaling exponents. Zhang [6] developed a simple analytical model that could explain several of the observed exponents for a particular universality class. These results were modified and extended by Christensen and Olami [7] and also by Robinson [8], who studied both scalar-field and vector-field SOC in addition to extending the analytic derivation to a number of other measurable exponents. Renormalization group methods have also been used by Vespignani *et al.* [9] and Ivashkevich [10] to make analytic estimates for exponents for a particular two-dimensional (2D) sandpile-type model.

To verify the theoretical results and to classify models into universality classes numerically it is necessary to obtain a wider range of exponents than has previously been done and to calculate both known and new exponents to a greater level of accuracy. Increasing the number and accuracy of known exponents will allow theoretical estimates to be tested more rigorously and allow for differentiation between models that lie in different universality classes but have exponents that are close to one another. An example of this was studied by Ben-Hur and Biham [11], who showed that the two-state model introduced by Manna [12] lay in a different universality class from the original Bak-Tang-Wiesenfeld (BTW) model [1], contrary to Manna's original claim. Many other models in use also have few accurately known exponents.

In this paper we improve the accuracy of known exponents for several models by increasing the size of previous numerical simulations. We also establish a wider range of exponents for existing models and increase the number of different models for which accurate exponents are known. In addition we test the theoretical interrelationships of Zhang [6], Christensen and Olami [7], and Robinson [8] and compare the analytical results of Vespignani *et al.* [9] and Ivashkevich [10] with numerical results. It is verified that for these models if two exponents are known, then the remaining exponents can be accurately determined analytically, provided the two chosen exponents collectively involve both spatial and temporal scalings. We also discuss differences between the continuous (real valued) Zhang [6] height-triggered model, the standard discrete (integer valued) BTW [13] height-triggered model, and the modified continuous model introduced by Diaz-Guilera [14]. Differences in the redistribution rule causes different distributions of the field on the lattice [14] and break-point behavior in some of the exponents. Despite this the dynamic exponents of the different models appear to lie in the same universality class.

In Sec. II we introduce the SOC models considered in this work. In Sec. III we discuss scaling exponents and the theoretical relationships between them. In Sec. IV we present the results of numerical simulations and discuss their implications. Our results in this section are compared with previous simulations, theoretical interrelationships and renormalization group estimates. We conclude in Sec. V.

II. MODELS

In this section we outline the SOC models considered in this paper. All the models involve driving and relaxation of a field that is analogous to the sand in a sandpile. SOC models

*Electronic addresss: edney@physics.usyd.edu.au

must involve three features [13]. (i) The system must be driven via the addition of field increments (e.g., grains of sand). (ii) The system must have a local critical triggering condition such that when a region satisfies the condition it relaxes (e.g., in a sandpile, if the slope at a particular point becomes too great, the sand will slide to neighboring regions). (iii) The system must be able to relax and return itself to below the critical condition, by redistributing the field to neighboring regions and conserving a quantity analogous to the energy of the field (e.g., in a sandpile sand slides until it settles in positions such that the slope is everywhere less that the critical slope).

The SOC models used here are cellular automatons on two- or three-dimensional square or cubic grids of side N, on which a D-component continuous vector field $\mathbf{F}$ is defined at each point. Our models differ from the majority of similar models in the literature [7,12,13,15] in that our models use the continuous field model introduced by Zhang [6] and a random component to the field increment. The models are driven by adding a field increment $\mathbf{g}$ at a randomly chosen site, with

$$\mathbf{F}\rightarrow\mathbf{F}+\mathbf{g} \tag{1}$$

at this site. The increment is a random variable with mean values of its various components given by

$$\langle g_n\rangle=\begin{cases}\mu, & n=1\\ 0, & n>1,\end{cases} \tag{2}$$

where μ is a constant. Each component of $\mathbf{g}$ also has an additive random part uniformly distributed between $-\Delta$ and Δ. The component g_1 is chosen to be the only component with a nonzero mean. This can be done without loss of generality because a coordinate rotation can always be made to bring $\langle\mathbf{g}\rangle$ into the form (2). In this work we only consider models with a two-component vector field.

In this paper we primarily examine models with two different relaxation conditions. The first relaxation condition, described as height triggered, is satisfied when the addition of a field increment causes $|\mathbf{F}|$ to exceed a critical value (in the sandpile case this corresponds to the height of the pile exceeding a critical value). This model is the same as the model introduced by Zhang [6]. The second relaxation condition, described as curvature triggered, is satisfied when the magnitude of the local field ''curvature'' ($|\nabla^2\mathbf{F}|$ in the continuum limit) becomes greater than a critical value. In the discrete case the quantity $\Phi(\mathbf{F}_i)$, which plays the role of curvature, is defined on a d-dimensional square or cubic grid by

$$\Phi(\mathbf{F}_i)=\mathbf{F}_i-\sum_{n,n}\frac{\mathbf{F}_{nn}}{2d}, \tag{3}$$

which is the discrete analog of $\nabla^2\mathbf{F}$. In both cases the field is redistributed so that the quantity upon which the triggering is based ($|\mathbf{F}|$ for height triggering and $|\Phi(\mathbf{F}_i)|$ for curvature triggering) would be reset to zero in the absence of any other relaxations. This is done in the height-triggered case by redistributing the field equally to the 2D neighboring sites on a d-dimensional rectangular grid. In the case of curvature triggering the field is redistributed by setting

$$\mathbf{F}_{nn}=\mathbf{F}_{nn}-\frac{2d}{2d+1}\Phi(\mathbf{F}_i), \tag{4}$$

$$\mathbf{F}_i=\mathbf{F}_i+\frac{1}{2d+1}\Phi(\mathbf{F}_i), \tag{5}$$

which also conserves the field.

Relaxation of an unstable site may cause adjacent sites to become unstable and these locations will then also relax. An avalanche of relaxations can thus occur that is allowed to proceed until all sites are stable before the next field increment is added.

Our work on both curvature-triggered and height-triggered models uses open boundary conditions with $\mathbf{F}=\mathbf{0}$ on the boundary, beyond which the field is lost to the system. In the numerical work in Sec. IV we examine the eight different models obtained by considering two and three dimensions, vector and scalar cases, and height and curvature triggering. In order to gauge the effects of slight changes to the redistribution rules, we also examine a variation of the continuous Zhang [6] height-triggered model, introduced by Diaz-Guilera [14]. Instead of resetting the field at an unstable site to zero, this model reduces the field by the critical value and redistributes the critical field equally among the 2D neighboring sites. This model corresponds more closely to the redistribution rules of the original discrete BTW [13] model and is discussed in more detail in Sec. IV.

III. THEORY

In this section we define the physical quantities whose scalings are of interest. We also briefly review the theoretical interrelationships between their scaling exponents. In Sec. IV these relationships are tested against numerical results for the eight models introduced in Sec. III.

The physical quantities of interest to us all measure aspects of avalanches triggered when an initial site becomes unstable and distributes the field to neighboring sites, which may then also relax. We consider the processes beginning when one site becomes unstable and ending when all sites become stable again to constitute a single avalanche. The following physical quantities are defined for each avalanche. (i) The area a is the total number of different sites that become unstable (active). (ii) The total number of activations of sites is s. This differs from the area in that it accounts for multiple activations of some sites. (iii) The duration is t. This is the number of iterations necessary to allow the system to relax to an stable configuration. (iv) The radius r is defined to be [8]

$$r=r_0+\frac{1}{2d}\sum_{i=1}^{d}[\max(R_i)-\min(R_i)], \tag{6}$$

where R_i is the ith component of R and the maxima and minima are taken over all active sites (at locations $\mathbf{R}$). This definition uses the ''taxicab'' metric to determine the distance between the furthest separated points in the avalanche. This will give the correct radius for a spherical avalanche,

but will differ by a factor of $(2d)^{-1}$ for a (rare) straight line avalanche, consisting of a single line of active sites. The r_0 term adjusts the radius so that a single element avalanche has radius equal to the radius of a spherical avalanche of unit volume, but has negligible effect for large avalanches [8]. (v) The maximum power p is defined as the maximum number of sites simultaneously active during the avalanche.

A number of theoretical interrelationships between SOC scaling exponents have been derived by Zhang [6], Christensen and Olami [7], and Robinson [8]. These allow the calculation of the full range of exponents from only two measured ones. We define a set of exponents α_Q to describe the scaling of the probability distribution $D(Q)$ of some avalanche quantity Q, with

$$D(Q) \sim Q^{1-\alpha_Q}. \tag{7}$$

For the special case of the area exponent α_a we write $\alpha_a = \tau$, which is consistent with previous notation. A second set of exponents δ_Q relates the different physical quantities to the area a. These are defined by

$$Q \sim a^{\delta_Q}. \tag{8}$$

We may also define the dynamic exponent found by many previous authors by

$$z = \frac{\delta_t}{\delta_r}. \tag{9}$$

If the exponents τ and α_Q are known then it is also possible to determine the value for δ_Q, giving [8]

$$\delta_Q = \frac{\tau - 2}{\alpha_Q - 2}. \tag{10}$$

Below the critical dimension we may treat the avalanches as spatially compact objects. Doing this one finds the relationship $a \sim r^d$ between the area a and radius r, giving $\delta_r = 1/d$. It is then possible to express all the exponents for these models, below the critical dimension, in terms of any two measured exponents, as long as the two exponents chosen collectively involve at least [6,8] one spatial and one temporal characteristic of the system. We can thus express all exponents in terms of τ and α_t, for example.

The power p can be expressed as the time derivative of the total number of activations at the boundary of the avalanche as the area increases, plus the increase due to old sites reactivating [6,8]. For small avalanches the activations on the boundary dominate, while for larger avalanches reactivations account for the majority of the number of total activations. This results in a change in the physics between the two regimes and causes breakpoints to appear in the scalings of a, p and related quantities.

If we take τ and α_t as our two basic exponents we find the interrelationships [6–8]

$$\alpha_s = \begin{cases} \tau, & a \text{ small} \\ \dfrac{\tau d + 2}{d+1}, & a \text{ large,} \end{cases} \tag{11}$$

$$\alpha_r = 2 + d(\tau - 2), \tag{12}$$

$$\alpha_p = \begin{cases} \dfrac{\tau(\alpha_t - 4) + 4}{\alpha_t - \tau}, & p \text{ small} \\ \dfrac{\tau d(\alpha_t - 4) + 2(\alpha_t - 2) + 4d}{\alpha_t - 2 + d(\alpha_t - \tau)}, & p \text{ large,} \end{cases} \tag{13}$$

$$\delta_t = \frac{\tau - 2}{\alpha_t - 2}, \tag{14}$$

$$\delta_p = \begin{cases} \dfrac{\alpha_t - \tau}{\alpha_t - 2}, & p \text{ small} \\ \dfrac{d+1}{d} - \dfrac{\tau - 2}{\alpha_t - 2}, & p \text{ large,} \end{cases} \tag{15}$$

$$\delta_s = \begin{cases} 1, & a \text{ small} \\ \dfrac{d+1}{d}, & a \text{ large,} \end{cases} \tag{16}$$

$$\delta_r = \frac{1}{d}. \tag{17}$$

IV. NUMERICAL RESULTS

We have simulated the models outlined in Sec. III using cellular automatons on square and cubic grids. We review the basis of these calculations in Sec. IV A and present the results for height-triggered and curvature-triggered models in Secs. IV B and IV C, respectively.

A. General

The models studied here were driven until a statistical equilibrium developed between driving and relaxation. This was achieved by ensuring that the average mass over time was constant. Curvature-triggered models took longer to come to equilibrium than the comparable height-triggered models, with the largest models requiring the order of 1000 times as many field increments to be added to become stable compared to the height-triggered models. This is consistent with the result that height-triggered models need $O(N^2)$ increments to come to equilibrium, whereas curvature-triggered models typically require $O(N^4)$, as found by Manna [19], despite the slightly different relaxation rule. As a result, curvature-triggered models were necessarily run on smaller grid sizes. The distributions are generated by looking at 10^5 avalanches for most grid sizes, with double this being used for the largest grid sizes for each model.

While exponents of sandpiles with larger grid sizes than presented here have been reported [11,15,16] previously, it should be noted that, with the exception of the 2D height triggered model [16], these have been for discrete models and not for the continuous height- and curvature-triggered models studied here. The latter are more physically realistic models of continuous systems. The question of whether they are in the same universality class as discrete ones (for which there is considerable evidence [6,8,16,17]) is a question that has to be settled elsewhere by numerical simulations of both types.

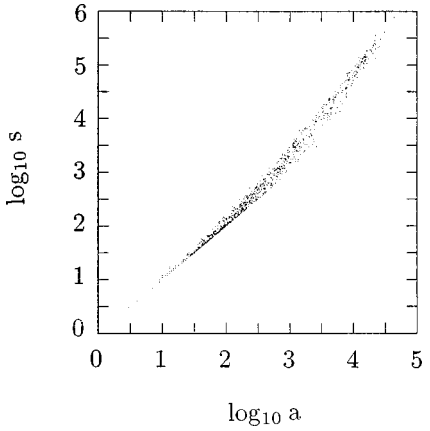

FIG. 1. Scatter plot of the number of activations s versus area a for the 2D height-triggered model.

The exponent δ_Q is obtained by plotting the values of an avalanche quantity Q against the corresponding values of area a from the largest size model, producing a scatter plot like that shown in Fig. 1. Because of the high density of results in the small-a range of the scatter plots it is necessary to weight the fit so that each range of area contributes equally to the fit and it is not dominated by the numerous small-a data. The exponent α_Q is determined from a distribution obtained by binning the Q values of many avalanches against Q as shown in Fig. 2. The critical exponents for each size model are determined by least-squares fits to these plots. Each fit is made to a suitable subrange of the available data so that the upper and lower scales of the model, and any breakpoint, do not strongly affect the calculated exponent. It has been noted by other authors that the measured exponents are a function of the system size [15,16,18,19], with $\alpha_\infty = \alpha_N + k/N^n$, where α_N is the exponent measured at a particular grid size N. Fitting our finite-N results to an expression of this form, we can extrapolate to obtain α_∞ as in Fig. 3. It has been found by Ben-Hur and Biham [11] that the δ exponents are not strongly effected by system size (a conclusion that our results support), so extrapolation is not necessary; instead, the exponent from the largest simulation is used. The effect of a breakpoint can be seen in Fig. 1; here we obtain the upper (large avalanches) and lower (small avalanches) exponents by performing the least-squares fit over each region separately. We denote the exponents by the subscripts u and l, respectively.

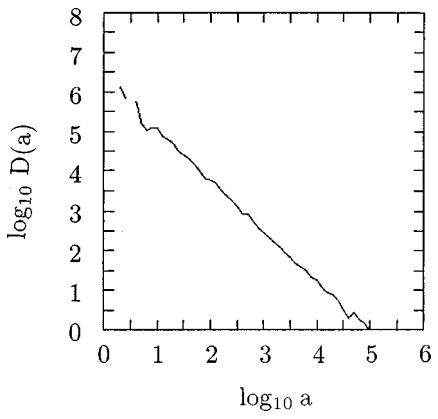

FIG. 2. Unnormalized distribution $D(a)$ of the area a for the 2D height-triggered model.

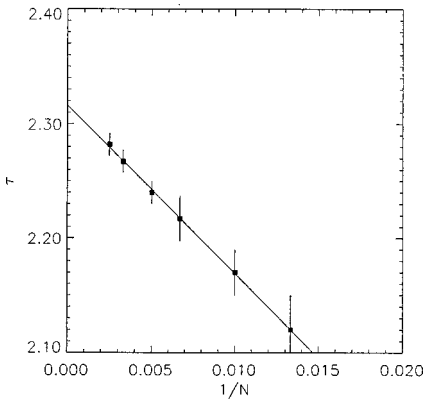

FIG. 3. Extrapolation of the τ for the scalar 2D height-triggered model.

B. Height-triggered models

In this section we discuss the differences between several continuous and discrete 2D models and their effects on SOC physics before presenting our results for the continuous Zhang model in detail.

1. Comparison of continuous and discrete 2D models

The continuous height-triggered models primarily studied here were introduced by Zhang [6] and have previously been found to have exponents that lie in the same universality class as the original discrete BTW height-triggered model [6,8,14,15]. However, Diaz-Guilera [14] noted that the Zhang model is not just a continuous version of the original BTW model. In the Zhang model, the field at a site that relaxes is reduced to zero, whereas in the BTW model the field at an active site is reduced only by the critical value and so in some cases may have a nonzero field remaining after relaxation. Diaz-Guilera [14] found that making this change to the Zhang model caused large differences in the distribution of the field on the lattice, but, despite noting that the BTW model contains an extra symmetry in the redistribution rules, could not find any significant differences in exponents of his numerical simulations. Using an effective-medium method, Diaz-Guilera also showed analytically [20] that the two models should lie in the same universality class despite the extra symmetry in the BTW model. In contrast, more recent work by Blanchard *et al.* [21] implies that models where a fixed value of the field is transferred in a relaxation (BTW) should have different properties from models where the whole field is redistributed on relaxation (Zhang).

One difference between the BTW and Zhang models is the existence or lack of breakpoints in the observed power laws. As mentioned previously, Robinson [8] found breakpoints in the power laws underlying some of the exponents of the Zhang model, notably $\delta_s \approx 1$ for $a \leqslant 100$ and $\delta_s \approx 1.5$ for $a \geqslant 1000$. The breakpoints in the power laws were found to be independent of grid size and hence a real feature of the dynamics. The present work reconfirms these results. Corresponding simulations performed both here and by others [11,15] do not find this kind of breakpoint behavior in the standard BTW model. Similarly, using the modified Zhang

TABLE I. Numerically calculated critical exponents and other quantities for height-triggered models. Column 1 is taken from Lübeck and Usadel [18].

Quantity	Value				
d	2	2	2	3	3
field	scalar	scalar	vector	scalar	vector
N	2048	400	400	80	80
τ	2.338 ± 0.015	2.32 ± 0.03	2.30 ± 0.04	2.34 ± 0.03	2.35 ± 0.02
α_t		2.41 ± 0.04	2.38 ± 0.06	2.61 ± 0.03	2.60 ± 0.03
α_{p_l}		2.85 ± 0.06	2.79 ± 0.06	2.81 ± 0.03	2.83 ± 0.04
α_{p_u}		2.40 ± 0.06	2.43 ± 0.03		
α_s	2.282 ± 0.010	2.29 ± 0.03	2.29 ± 0.04	2.34 ± 0.03	2.34 ± 0.03
α_r	2.682 ± 0.018	2.58 ± 0.05	2.53 ± 0.06	2.50 ± 0.05	2.55 ± 0.06
δ_t		0.61 ± 0.04	0.60 ± 0.04	0.53 ± 0.04	0.54 ± 0.04
δ_{p_u}		0.96 ± 0.06	0.99 ± 0.06	0.61 ± 0.07	0.62 ± 0.08
δ_{p_l}		0.54 ± 0.08	0.54 ± 0.09	0.56 ± 0.05	0.55 ± 0.07
δ_{s_u}		1.54 ± 0.06	1.57 ± 0.06	1.15 ± 0.05	1.13 ± 0.05
δ_{s_l}		1.01 ± 0.02	1.01 ± 0.02	1.01 ± 0.01	1.00 ± 0.01
δ_r		0.49 ± 0.02	0.49 ± 0.02	0.35 ± 0.02	0.36 ± 0.02
Universality class	A	A	A	B	B

model proposed by Diaz-Guilera [14], we find plots almost identical to the standard BTW model for s vs a. Thus breakpoints seem to be a feature of the Zhang relaxation rule ($E\rightarrow0$) for unstable sites, but do not appear for the BTW relaxation rule ($E\rightarrow E-E_c$).

To further explore the δ_s exponent we look at the conditional probability distribution $P(s|a)$. Lübeck and Usadel [15] found that for the discrete BTW model $P(s|a)$ was distributed asymmetrically against the boundary $s=a$. This meant that the scaling relationship $s\sim a^{\delta_s}$ was not well defined since this relationship requires the conditional probability $P(s|a)$ to be strongly peaked around the expectation value $E(s|a)$. In our simulations of the Zhang model we find that in regions below the breakpoint the conditional probability is strongly peaked where $s=a$ and is therefore asymmetric as in the BTW case. For values of a above the breakpoint, however, we find that $P(s|a)$ is peaked strongly and symmetrically around the expectation value $E(s|a)$ and therefore the exponent is well defined in this region.

Although substantial differences do occur between the Zhang model and the BTW model, particularly with regard to the existence of breakpoints in power-law distributions at small a, there is considerable evidence [11,16] that the dynamic exponents at large a imply that both models belong to the same universality class (see below for a comparison). In the remainder of this work we look at continuous models that trigger when a site becomes unstable and relaxes completely. For height-triggered models this corresponds to the Zhang model.

2. Exponents determined from our simulations

In this section we discuss results from 2D and 3D, scalar and vector height-triggered models. The 2D models are simulated on grid sizes up to 400×400 and the corresponding 3D models are simulated on a grid sizes up to $80\times80\times80$. This means that the typical maximum area of an avalanche will be larger in the 3D case than in the 2D case; however, the maximum radius will be smaller in the 3D case. The results in Table I show the exponents obtained from numerical simulations of the four height-triggered models. Note that the quoted error values are the maximum of the standard deviation of the slope of the line from the least-squares fit and the typical variation in the exponent measured over successive long time intervals. Fluctuations persist even on the longest time scales owing to the power-law temporal correlations in the SOC state. For the scalar 2D height-triggered model we also include the results of Lübeck [16] for some exponents for comparison since these are obtained on a larger grid size than ours.

As in [16] we find that the exponent varies as $\tau_N=\tau_\infty+k/N^n$ with $n=1$ for the 2D height-triggered model. We use six different grid sizes (50, 100, 150, 200, 300, and 400) for the 2D height-triggered models to determine the extrapolated exponents. For the 3D height-triggered models we find that $n=2$ gives the best fit to a straight line and we use five different grid sizes (10, 20, 30, 50 , and 80) to extrapolate from. The extrapolated exponent for τ for the scalar 2D height-triggered model is shown in Fig. 3.

In the 2D scalar case many of the exponents in Table I can be compared with ones determined by previous authors. The value $\tau=2.32\pm0.03$ obtained here is in good agreement with the value $\tau=2.338\pm0.015$ obtained by Lübeck using larger simulations [16]. The values are larger than the earlier results of Robinson [8] ($\tau=2.22\pm0.05$) and Janosi [17] ($\tau=2.2$), but this is to be expected since those were obtained using smaller grid sizes and were not extrapolated to find the value at infinite grid size. Vespignani *et al.* found a value $\tau=2.254$ [9] and Ivashkevich found $\tau=2.248$ [10] using renormalization group methods. Both these estimates appear to be too low based on the results here and other published results [15,16].

From Table I and Eq. (9) we find a value for the dynamic exponent $z=1.24\pm0.05$. This differs from the value of z

TABLE II. Numerically calculated critical exponents and other quantities for curvature-triggered models.

Quantity	Value			
d	2	2	3	3
field	scalar	vector	scalar	vector
N	200	200	80	80
τ	2.42 ± 0.03	2.45 ± 0.03	2.47 ± 0.02	2.47 ± 0.02
α_t	2.59 ± 0.03	2.64 ± 0.03	2.69 ± 0.04	2.68 ± 0.04
α_p	2.63 ± 0.05	2.73 ± 0.05	3.03 ± 0.05	3.01 ± 0.10
α_s	2.33 ± 0.03	2.36 ± 0.04	2.47 ± 0.04	2.47 ± 0.04
α_r	2.65 ± 0.05	2.73 ± 0.05	2.81 ± 0.05	2.82 ± 0.05
δ_t	0.79 ± 0.04	0.79 ± 0.04	0.59 ± 0.03	0.59 ± 0.03
δ_p	0.76 ± 0.04	0.75 ± 0.04	0.59 ± 0.07	0.59 ± 0.04
δ_{s_l}	1.10 ± 0.05	1.11 ± 0.06	1.03 ± 0.02	1.02 ± 0.02
δ_{s_u}	1.59 ± 0.03	1.58 ± 0.04		
δ_r	0.51 ± 0.02	0.50 ± 0.02	0.38 ± 0.02	0.34 ± 0.02
Universality class	C	C	D	D

$=(d+2)/3$ found analytically by Zhang [6] and Diaz-Guilera [14], but is in agreement with the value of $z=\frac{5}{4}$ found by Majumdar and Dhar [22] using the equivalence between the sandpile and the $q \to 0$ limit of the Potts model.

Table I shows that almost all the exponents of the 2D vector height-triggered model are the same as those for the scalar model to within uncertainties (the only marginally significant difference occurs in α_r where the two values lie just outside each others uncertainties). This indicates that the vector model lies in the same universality class as the scalar model, in agreement with the conclusions of Robinson [23]. (Note that we neglect the difference in the α_{p_l} values because these pertain only to small avalanches.)

There are fewer existing results for the 3D height-triggered models in the literature than for the equivalent 2D models. The results of Robinson [8] are in agreement with the improved exponents presented here to within the uncertainties. The value $\tau=2.35$ obtained by Bak *et al.* [13], $\tau=2.35$ and $\delta_t=0.56$ obtained by Ben-Hur and Biham [11], and $\tau=2.33$ obtained by Lübeck and Usadel are also consistent with the values displayed in Table I. A much higher value for $\tau=2.55$ was found by Janosi [17], but this was obtained using a much smaller grid than was used in obtaining the other results. It is seen that $\tau \approx \alpha_s$, also in agreement with previous work [11,18]. With the exception of Robinson [8] and Janosi [17], these simulations were of discrete models, so these results support the claim that the continuous and discrete models lie in the same universality class. No break points, such as were observed clearly in the continuous 2D models, are seen in the 3d models. This extends the claim of [18] that $\tau=\alpha_s$ for discrete 3D models to also cover continuous 3D models.

As in the 2D case, the 3D vector height-triggered model has scaling exponents that indicate that it lies in the same universality class as the corresponding scalar model. This is again in agreement with the results of Robinson [23].

The theoretical predictions (10)–(16) of Zhang [6], Christensen and Olami [7], and Robinson [8] accurately predict the range of exponents for the 2D height-triggered models, both scalar and vector, in terms of α_t and τ with the exception of δ_p and α_p, where the agreement is poorer. These latter exponents are the most uncertain in our simulations due to the relatively short power laws generated. The existence of a poorly defined breakpoint also complicates the numerical analysis. Hence the apparent discrepancies may reflect these numerical uncertainties rather than real differences.

The exponents for the 3D models do not satisfy Eqs. (10)–(16) as closely as those in 2D models. Significant deviations occur in δ_p, δ_{s_u}, α_r, and α_{s_u}. These discrepancies may be the result of power-law fits being restricted to small ranges or poorly defined breakpoints, as suggested above for the 2D case. In particular, α_r is more poorly defined numerically in the 3D models than the 2D models because of the shorter linear scale of the model. The disagreement in the α_{s_u} exponent may be caused by the finite size of the model cutting off the power law before the upper exponent completely develops.

C. Curvature-triggered models

The exponents for curvature-triggered models are shown in Table II in the same format as Table I. The simulations are performed on smaller grids than their comparable height-triggered counterparts due to the much longer period of time required for curvature-triggered models to reach a steady state. Breakpoints in α_p and δ_p were not apparent for the curvature-triggered models, so only one exponent is listed for each quantity in Table II.

To determine the extrapolations to obtain infinite-system exponents we use five different grid sizes (50, 75, 100, 150, and 200) for the 2D curvature-triggered models and (10, 20, 30, 50, and 80) for the 3D curvature-triggered models. Again, as in the height-triggered models, we find that $n=1$ gives the best fit for the 2D models and $n=2$ for the 3D models.

Table II shows the results for the curvature-triggered models. It can be seen that both the scalar and vector models

TABLE III. Comparison of critical exponents for the 3D curvature-triggered model, obtained by Lu *et al.* [24] and in the present work.

Exponent	Lu *et al.*	Present work
α_t	2.88	2.68 ± 0.04
α_s	2.51	2.45 ± 0.04
α_p	2.86	3.03 ± 0.05

have exponents generally match to within each other's limit of error. There are some discrepancies in the 2D models for α_p and α_r, which have only overlapping uncertainties; however, these exponents, as noted earlier, are the most inaccurately measured in our models. These results then are consistent with the models lying in same universality class for a given d. This result extends to curvature-triggered models Robinson's [23] conclusion that scalar and vector height-triggered models of given d were in the same universality class. A comparison of Tables I and II shows that height-triggered and curvature-triggered models of a given D lie in different universality classes.

Fewer values for exponents for curvature-triggered models have been previously published than for height-triggered models. The 2D curvature-triggered model has been examined by Kadanoff *et al.* [5] and Manna [19]; however, it must be noticed that both these models used a different relaxation rule from the one used here. In analogy to the Zhang model for height triggered sandpiles, we reduce the curvature at the relaxed site to zero, whereas Kadanoff *et al.* [5] and Manna [19], in analogy with the BTW height-triggered model [1], reduced the curvature at the critical site by a constant amount (see Sec. IV B for a comparison with the height-triggered case).

Manna found values $\alpha_s = 2.3$, $\alpha_t = 2.57$, and an exponent $x = \delta_t / \delta_s = 0.53$ in our notation. These appear to be consistent with our results of $\alpha_s = 2.36 \pm 0.04$, $\alpha_t = 2.62 \pm 0.05$, and $x = \delta_t / \delta_s = 0.52$, particularly as Manna did not quote uncertainties in the former results. Most of the exponents of Kadanoff *et al.* [5] are not comparable to the ones used here; however, they did obtain $\alpha_s = 2.50 \pm 0.10$, which is larger than the values presented here. This discrepancy appears to be the result of the smaller maximum grid size ($N = 64$) used in their work and is consistent with the trend in our work.

For the 3D curvature-triggered case some exponents have been calculated numerically by Lu *et al.* [24] and are compared to the present ones in Table III. These exponents match reasonably closely in the case of α_a, falling just inside the error quoted in our results. In the cases of α_t and α_p, the values of Lu *et al.* [24] lie well outside our quoted error. However, if we compare models of the same sizes we find that the correspondence for each between the models is closer, especially in the case of α_t. Lu *et al.* [24] gave results only for a specific grid size for each of their models and no error estimates on their values, so it is difficult to judge exactly how close a match these values are. If there is a discrepancy its cause is still unclear, but may be due to an undetected breakpoint in the α_p plots in the model of Lu *et al.* [24] or ours. Such a breakpoint would lead to values of exponents intermediate between the true upper and lower ones and similar to the ones actually seen here.

The theoretical predictions of Zhang [6], Christensen and Olami [7], and Robinson [8] do not in general give as accurate predictions for exponents of the curvature-triggered models as for those of the height-triggered models. In the 2D models we find that predictions of α_p, δ_p, and α_r are particularly poor, while numerical and theoretical values of α_r, α_s, and δ_t differ by slightly more than the quoted errors. The 3D exponents agree better with the theory, but the agreement is still poor in several cases, particularly for δ_r, which, as mentioned earlier, is less well defined in the 3D models. There is also some disagreement for δ_p and δ_t, which differ from theoretical estimates by slightly more than their estimated errors. It appears that the exponents in the 3D models are particularly affected by the relatively small system size. Larger systems will be required to obtain more accurate verification of the results of Zhang [6], Christensen and Olami [7], and Robinson [8].

V. CONCLUSION

Extensive numerical simulations of eight sandpile type SOC models have been carried out and their scaling exponents have been determined in a uniform way. In all cases except the 2D height-triggered model, our simulations have been carried out of grids larger than in previous works for these models. The 2D height-triggered results of Lübeck [16] have also been included for completeness as they are obtained on larger grid sizes. We also discuss differences between the Zhang [6] model and the BTW model [1], in particular the appearance of breakpoint behavior in some exponents of the Zhang model.

Our results for scaling exponents are in general agreement with other published values including those of Lübeck [16] and in most cases have been calculated to a greater degree of accuracy than in previous work. Unlike many previously published results, our results also include uncertainty estimates, which allow a clearer comparison between the exponents we have determined and values determined elsewhere in the literature.

One of our major conclusions is that scalar and vector models lie in the same universality class for both height-triggered and curvature-triggered cases. This generalizes Robinson's [23] results for height-triggered models to the curvature-triggered case. In contrast, a change from height- to curvature-triggering does change the universality class, as does a change from two- to three-dimensional systems for either type of triggering.

In both the 2D height- and curvature-triggered models we find that there is a difference between the exponents τ and α_s. This difference does not appear in the 3D models where $\tau = \alpha_s$. In the 2D height-triggered model we find that, while the dynamic exponents tend to be the same as in the discrete BTW model, there are differences in the δ_a exponent.

The numerically derived scaling exponents were compared with the theoretical estimates from Eqs. (9)–(16) derived on the basis of various scaling assumptions [6–8]. Only in the 2D height-triggered model do we find compel-

ling agreement between the numerically derived exponents and the theoretical predictions (10)–(16). In the 3D height-triggered and the 2D and 3D curvature-triggered models the majority of the exponents are consistent with theoretical predictions; however, there are discrepancies in some exponents. The largest discrepancies occur for the exponents that are least well determined numerically, whereas the numerically better-defined exponents are predicted correctly. This suggests that the remaining discrepancies may be resolvable by larger-scale simulations in the future.

ACKNOWLEDGMENTS

This work was supported by the Australian Research Council. S.D.E. was supported by the Australian Postgraduate Award Scheme.

[1] P. Bak, C. Tang, and K. Wiesenfeld, Phys. Rev. Lett. **59**, 381 (1987).
[2] J. M. Carlson and J. S. Langer, Phys. Rev. Lett. **62**, 2632 (1989).
[3] E. Lu and R. Hamilton, Astrophys. J. **380**, L89 (1991).
[4] D. A. Noever, Phys. Rev. E **47**, 724 (1993).
[5] L. Kadanoff, S. Nagel, L. Wu, and S. Zhou, Phys. Rev. A **39**, 6524 (1989).
[6] Y. C. Zhang, Phys. Rev. Lett. **63**, 470 (1989).
[7] K. Christensen and Zeev Olami, Phys. Rev. E **48**, 3361 (1993).
[8] P. A. Robinson, Phys. Rev. E **49**, 1984 (1994).
[9] A. Vespignani, S. Zapperi, and L. Pietronero, Phys. Rev. E **51**, 1711 (1995).
[10] E. V. Ivashkevich, Phys. Rev. Lett. **76**, 3368 (1996).
[11] A. Ben-Hur and O. Biham, Phys. Rev. E **53**, 1317 (1996).
[12] S. S. Manna, J. Phys. A **24**, L363 (1991).
[13] P. Bak, C. Tang, and K. Wiesenfeld, Phys. Rev. A **38**, 364 (1988).
[14] A. Diaz-Guilera, Phys. Rev. A **45**, 8551 (1992).
[15] S. Lübeck and K. D. Usadel, Phys. Rev. E **55**, 4095 (1997).
[16] S. Lübeck, Phys. Rev. E **56**, 1590 (1997).
[17] I. M. Janosi, Phys. Rev. A **42**, 769 (1990); **88**, 307 (1997).
[18] S. Lübeck and K. D. Usadel, Phys. Rev. E **56**, 5138 (1997).
[19] S. S. Manna, Physica A **179**, 249 (1991).
[20] A. Diaz-Guilera, Europhys. Lett. **26**, 177 (1994).
[21] Ph. Blanchard, B. Cessac, and T. Krüger, J. Stat. Phys. **88**, 307 (1997).
[22] S. N. Majumdar and D. Dhar, Physica A **185**, 129 (1992).
[23] P. A. Robinson, Phys. Rev. E **49**, 3919 (1994).
[24] E. T. Lu, R. J. Hamilton, J. M. McTiernan, and K. R. Brodmund, Astrophys. J. **412**, 841 (1993).